Abdominal Imaging

Published online: 7 January 2009

Abdom Imaging (2010) 35:246–252
DOI: 10.1007/s00261-008-9495-2

Prostate MR imaging at 3T using a phased-arrayed coil in predicting locally recurrent prostate cancer after radiation therapy: preliminary experience

Chan Kyo Kim,[1,2] Byung Kwan Park,[2] Won Park,[3] Sam Soo Kim[1]

[1]Department of Radiology, Kangwon National University College of Medicine, Chuncheon, Republic of Korea
[2]Department of Radiology and Center for Imaging Science, Samsung Medical Center, Sungkyunkwan University School of Medicine, 50 Ilwon-dong, Kangnam-gu, Seoul 135-7100, Republic of Korea
[3]Department of Radiation and Oncology, Samsung Medical Center, Sungkyunkwan University School of Medicine, Seoul, Republic of Korea

Abstract

The purpose of this study was to retrospectively assess the diagnostic performance of diffusion-weighted imaging (DWI) and dynamic contrast-enhanced imaging (DCEI) at 3T in predicting locally recurrent prostate cancer after radiation therapy. Twenty-four patients with a rising prostate-specific antigen level after treatment with radiation therapy underwent prostate MR imaging at 3T, followed by transrectal ultrasound-guided biopsy. MRI findings and biopsy results were correlated in six prostate sectors of both peripheral zones. Two radiologists in consensus reviewed the MR images and rated the likelihood of recurrent cancer on a 5-point scale. Out of the 144 prostate sectors, 37 (26%) sectors were positive for cancer in ten patients. For predicting locally recurrent cancer, the sensitivity and specificity of DWI, DCEI, and combined DCEI and DWI were higher than those for T2-weighted imaging (T2WI). The accuracy of DWI, DCEI and combined DCEI and DWI was greater than that of T2WI. A significantly greater Az was determined for combined DCEI and DWI (Az = 0.863, $P < 0.05$) as compared with T2WI, DCEI, and DWI. For predicting locally recurrent prostate cancer after radiation therapy, our preliminary results suggest that the use of either DWI or DCEI is superior to the use of T2WI.

Correspondence to: Chan Kyo Kim; *email:* chankyokim@skku.edu

Key words: Prostate neoplasms—Radiotherapy—Diffusion-weighted MR imaging—Dynamic contrast-enhanced MR imaging—Local neoplasm recurrence

Biochemical failure after radiation therapy occurs in about 30%–50% of patients within 5 years [1, 2]. However, the management of locally recurrent prostate cancer after radiation therapy is limited. Exposure to further radiation is hazardous and risks serious injury to the rectum, bladder, or urethra [3]. Hormonal therapy usually provides tumor control that is effective but with limited duration [4]. A salvage radical prostatectomy can result in prolonged disease-free survival, but its routine use has not been widely accepted because of the inaccuracy of local staging and a tendency for clinical understaging prior to surgery [4, 5]. After definitive radiation therapy for localized prostate cancer, the level of serum prostate-specific antigen (PSA) is a reliable indicator of disease status, but it cannot distinguish between local and distant recurrence [4, 6].

An earlier diagnosis of locally recurrent prostate cancer and more accurate intraprostate mapping of the recurred prostate cancer after radiation therapy can provide a better selection of the appropriate second-line treatment. However, local tumor depiction with conventional T2-weighted MR imaging in the irradiated gland is limited by radiotherapy-related changes including diffused low T2 signal intensity in the gland and an indistinctness of the normal zonal anatomy, which is caused by glandular atrophy and fibrosis [7]. To date,

several investigations have demonstrated that dynamic contrast-enhanced imaging (DCEI) or spectroscopic imaging can improve the detection of locally recurrent prostate cancer after external beam radiation therapy [8–13]. To the best of our knowledge, however, the role of diffusion-weighted imaging (DWI) in the evaluation of recurred prostate cancer in patients with biochemical failure after external beam radiation therapy has not been investigated. More recently, 3T MR scanners have become commercially available. The increase in signal-to-noise ratio (SNR) with the use of a 3T scanner enables increased spatial and temporal resolution [14–17] and therefore a possible increase in accuracy of prostate cancer detection may be expected. Thus, the purpose of this study was to assess the diagnostic performance of the use of DCEI and DWI at 3T using a phased-array coil in predicting locally recurrent prostate cancer in patients with biochemical failure after the treatment with external beam radiation therapy.

Materials and methods

Patients

To be included in this study, a patient must have undergone the following: (a) prostate MR imaging (including DWI and DCEI) at 3T using a phased-array coil between January 2006 and April 2007 in our institution; (b) definitive external beam radiation therapy administered to the prostate prior to MR imaging; (c) a transrectal ultrasound (TRUS)-guided biopsy of the prostate performed in our institution within four months (mean, 28.9 days; range, 6–92 days) after MR imaging.

A total of 24 patients were identified and were included in the study population. These patients had biochemical failure after treatment with external beam radiation therapy. Biochemical failure was defined as three consecutive increases in the serum PSA level after a nadir [18]. The mean age of the 24 patients was 68 years (range, 57–77 years). All the patients that underwent external beam radiation therapy in our institution received a mean dose of 6750 cGy (range, 6600–7000 cGy). Five out of the 24 patients underwent adjuvant hormonal therapy after radiation therapy. The median interval from the completion of radiation therapy to MR imaging was 28 months (18.5–42.8 months). The mean PSA level prior to MR imaging was 2.76 ng/mL (range, 0.14–11.2 ng/mL).

The institutional review board approved this retrospective study and informed consent of patients was waived.

MR imaging

Prostate MR imaging was performed at 3.0 T (Intera Achieva 3T, Philips Medical System, Best, The Netherlands) by using a phased-array coil (six-channel). Before scanning, 20 mg of butyl scopolamine (Buscopan, Boehringer, Ingelheim, Germany) was injected intramuscularly to suppress the peristalsis of the bowel. No additional bowel preparation was performed. After obtaining three plane localizer images, T2-weighted turbo spin–echo images were acquired in the three orthogonal planes (axial, sagittal, and coronal). The scan parameters of the T2-weighted images were as follows: repetition time ms/echo time ms, 2600–4200/80; slice thickness, 3 mm; interslice gap, 0.3 mm; 512 × 304 or 304 × 304 matrix; field of view, 15–18 cm; number of signals acquired, 3; sensitivity encoding (SENSE) factor, 2. An axial T1-weighted turbo spin-echo sequence (4-mm slice thickness) was acquired to assess lymph nodes and the pelvic bone.

Axial diffusion-weighted images were obtained using the single-shot echo planar imaging technique with the following imaging parameters: repetition time ms/echo time ms, 2300–4400/63–65 ms; slice thickness, 3 mm; interslice gap, 1 mm; matrix, 112 × 112–110; FOV, 20 cm; SENSE factor 2; NSA, 4. Diffusion-encoding gradients were applied as a bipolar pair at b-values of 0 and 1000 s/mm^2, along the three orthogonal directions of the motion-probing gradients. Apparent diffusion coefficient (ADC) maps were automatically constructed on a pixel-by-pixel basis. The acquisition time of DWI was about 1 min and 32 s.

Axial dynamic contrast-enhanced images were obtained using a 3D-fast field echo sequence (repetition time ms/echo ms, 7.4/3.9; flip angle, 25°; matrix, 224 × 179; slice thickness, 5 mm; interslice gap, no; field of view, 20 cm; 11 partitions on a 3D slab). DCEI was scanned from the apex to the base of the prostate. The 3D volume with 11 partitions was acquired every 5 s and totally 58 scans were repeated. The dynamic acquisition consisted of one precontrast series and subsequent 57 postcontrast series. A postcontrast series was performed immediately after a bolus injection of gadopentetate dimeglumine (Magnevist, Schering, Germany) at a rate of 2 mL/s with a dose of 0.1 mmol/kg body weight using a power injector followed by a 15 mL saline flush. The total acquisition time for DCEI was approximately 5 min 22 s.

Transrectal prostate biopsy

A TRUS-guided biopsy was performed by two radiologists radiologists (B.K.P. and C.K.K. with 5 and 3 years of experience in prostate MR examination and TRUS-guided biopsy, respectively) in all the 24 patients with an 18-gauge needle mounted on a spring-loaded commercial biopsy device (Biopty Gun; Bard, Covington, GA, USA). Biopsy cores were obtained from every sextant including the medial and lateral aspect of base, medial and lateral aspect of midgland, and apex, with or without local anesthesia. If any recurred cancer was suspected in the prostate as seen at MRI, the two radiologists (B.K.P.

and C.K.K.) were asked to perform the targeted biopsy under TRUS guidance. All the biopsy cores were labeled to identify the biopsy location and all specimens were evaluated by one experienced uropathologist. The mean time interval between MR imaging and biopsy was 28.9 days (range, 6–92 days).

Image analysis

All the MR images were archived using a picture archiving and communication system (PACS; PathSpeed Workstation; GE Medical Systems, Milwaukee, WI). Two genitourinary radiologists (C.K.K., B.K.P.) who have had the experience of evaluating more than 600 prostate MR scans were asked to identify the presence or absence of cancer in the peripheral zone (PZ) of the six prostate sectors (base, midgland, and apex of each lobe) in consensus. The central gland was excluded in the analysis. The radiologists were aware that the patients had prostate cancer treated with external beam radiation therapy and rising PSA levels after radiation therapy but were unaware of all of the other clinical and histopathological findings.

Two readers in consensus made four separate readings. T2WI was analyzed in the first reading session, DWI was analyzed in the second reading session, DCEI were analyzed in the third reading session, and combined DCEI and DWI were analyzed in the fourth reading session. Images were randomly presented during each of the four reading sessions to avoid bias from learning effects. The time interval between each reading session was about 3 weeks.

Two readers visually reviewed the diffusion-weighted images and rated them in consensus for the degree of overall imaging quality. Overall imaging quality was rated as excellent, intermediate, or nondiagnostic. Quality was considered excellent if the images showed high spatial and contrast resolution and absence of susceptibility artifacts, or nondiagnostic if poor resolution and/or extensive susceptibility artifacts precluded adequate interpretation. Diffusion-weighted images that were not rated as either excellent or nondiagnostic were considered to be of intermediate quality.

The diagnostic criterion of locally recurrent prostate cancer in patients with biochemical failure after radiation therapy for T2WI was defined as a focal or mass-like hypointensity in the peripheral zone (PZ). Diffuse signal intensity at T2WI throughout the PZ was not considered as recurrent cancer. On DWI, a recurred cancer was considered when high focal signal intensities at $b = 1000$ s/mm^2 of DWI were demonstrated as low focal signal lesions relative to the surrounding PZ on ADC maps and their size was more than 5 mm in the transverse greatest diameter. At DCEI, the recurred cancer was defined as a focally hyperintense area relative to the surrounding PZ, especially within 60 s after a bolus injection of contrast material. Nonenhancement or ill-defined delayed gradual enhancement on DCEI was not considered as recurrent cancer.

Two readers in consensus subjectively rated the likelihood of a malignancy in the sextant sectors of both PZs of the prostate on using the following 5-point scale: (1) definitively absent; (2) probably absent; (3) possibly present; (4) probably present; (5) definitely present. When a score of three or higher was given, recurred prostate cancer was considered to be present.

Sextant tumor localization

After the completion of imaging assessment, the two radiologists (C.K.K. and B.K.P.) in consensus evaluated the location of recurrent cancer in the sextant prostate sectors of the PZ on the basis of histopathological findings of the biopsy. A sextant was considered positive at histopathological findings if it contained at least one tumor focus of biopsy cores.

Statistical analysis

Statistical analysis was performed with a statistical software package SAS software (version 8; SAS Institute, Cary, NC). For the prediction of locally recurrent prostate cancer, the sensitivity, specificity, positive predictive value (PPV), negative predictive value (NPV), and overall accuracy were calculated by dichotomizing the readings. A true-positive finding was considered in the case of a correlation of an imaging score of four or higher and the histopathological results for the prediction of locally recurrent cancer. The McNemar test was used to compare sensitivity and specificity values for each reading session. The Bonferroni correction was used to adjust for multiple comparisons, and a P value of less than 0.008 was considered to indicate a statistically significant difference. In the total 144 prostate sectors of 24 patients, the accuracy for each reading session was analyzed by using generalized estimation equations to account for clustering effects from multiple measurements in the same patient. The area under the receiver operating characteristic curve (Az) was calculated by using the scores for the prediction of locally recurrent cancer determined from T2WI, DCEI, DWI, and combined DCEI and DWI. Two-tailed tests were used to calculate all the P values. P values < 0.05 were considered as statistically significant for the comparison of Az values among imaging sequences.

Results

The mean number of biopsy cores obtained in patients was 11.5 (range, 10–14). A total of 144 prostate sectors of 24 patients were available for analysis. Out of the 144 prostate sectors, 37 (26%) were positive for cancer in ten

patients. Among these ten patients, eight patients had a bilaterally recurred cancer and the remaining two patients had a unilaterally recurred cancer. The Gleason score of the tumors ranged from six to nine (median, seven).

The overall image quality of DWI in 24 patients was as follows: excellent in 13 patients and intermediate in 11 patients. No image quality determined as nondiagnostic was found.

Table 1 presents the diagnostic performance of T2WI, DWI, DCEI, and combined DCEI and DWI at 3T using a phased-array coil in predicting locally recurrent cancer in sextant sectors of both PZs after radiation therapy (Figs. 1–2). The sensitivity and specificity for recurrent cancer detection were significantly higher for DWI (49% and 93%), DCEI (49% and 92%), and combined DCEI and DWI (59% and 91%) than for T2WI (27% and 80%) ($P < 0.008$). However, no statistical difference among DCEI, DWI, and combined DCEI and DWI was seen ($P > 0.05$). The accuracy in each of DWI (82%), DCEI (81%), and combined DCEI and DWI (83%) was greater than that for T2WI (67%) ($P < 0.001$). However, no statistical difference among DWI, DCEI and combined DCEI and DWI was found ($P > 0.05$).

The area under the receiver operating characteristic curve for the prediction of locally recurred cancer for T2WI, DCEI, DWI, and combined DCEI and DWI was 0.594, 0.737, 0.782, and 0.863, respectively (Fig. 3). The area under the receiver operating characteristic curve for DCEI, DWI, and combined DCEI and DWI was greater than that for T2WI ($P < 0.05$). A difference between DCEI and DWI was not found ($P = 0.336$). However, there was a statistical difference between combined DCEI and DWI and DWI ($P < 0.05$), and between combined DCEI and DWI and DCEI ($P < 0.05$).

Discussion

After external beam radiation therapy, the irradiated prostate gland shows diffused T2 low-signal intensity and indistinct zonal anatomy [7]. Thus, the tissue contrast between recurrent cancer and benign irradiated tissue is decreased as the recurrent cancer after radiation therapy demonstrates low signal intensity on T2WI. As was similar to a prior study using a 1.5T MR scanner [8], our results for T2WI at 3T using a phased-array coil showed a poor diagnostic performance in predicting recurrent cancer in patients with biochemical failure after radiation therapy.

In this study, the functional imaging methods of DCEI and DWI at 3T using a phased-array coil were used to predict locally recurrent prostate cancer in patients with biochemical failure after treatment with external beam radiation therapy. For the prediction of locally recurrent cancer, our preliminary results suggest that DWI, DCEI, and combined DCEI and DWI showed better sensitivity, specificity, and accuracy than T2WI and there were statistical significant differences. Therefore, these results of our study suggest that 3T prostate MR imaging using a phased-array coil may be useful after external beam radiation therapy in predicting local prostate cancer recurrence.

DCEI has been reported to be an effective tool in visualizing the pharmacokinetics of contrast material uptake in the prostate [19]. In a pretreatment evaluation of prostate cancer, DCEI has demonstrated enhancement patterns that are different from those of benign tissue [20, 21]. To date, to the best o four knowledge, only one investigation [8] at 1.5T using a phased-array coil has reported that for the depiction of recurred prostate cancer after radiation therapy, DCEI could predict locally recurrent cancer more accurately and with less interreader variability than T2WI. In their study[8], the specificity and accuracy in the PZ were 74%–85% and 74%–79%, respectively. However, in this study at 3T using a phased-array coil, the specificity and accuracy of DCEI were 93% and 83%, respectively. An explainable cause that could be demonstrated is that the increased SNR at 3T compared to 1.5T resulted in increasing the spatial and temporal resolution of DCEI, which could improve the diagnostic performance of detecting recurrent prostate cancer after radiation therapy. However, further investigations should be performed in large study populations.

Table 1. Diagnostic performance of prostate MR imaging at 3t using a phased-array coil in predicting locally recurrent cancer in sextant prostate sectors of both peripheral zones after radiation therapy

	T2WI	DCEI	P value*	DWI	P value†	DCEI + DWI	P value¶
Sensitivity (%)	27 (10/37)	49 (18/37)	0.008	49 (18/37)	0.008	59 (22/37)	<0.001
Specificity (%)	80 (86/107)	92 (98/107)	<0.001	93 (100/107)	<0.001	91 (97/107)	0.001
PPV (%)	32 (10/31)	67 (18/27)		72 (18/25)		69 (22/32)	
NPV (%)	76 (86/113)	84 (98/117)		84 (100/119)		87 (97/112)	
Accuracy (%)	67 (96/144)	81 (116/144)	<0.001	82 (118/144)	<0.001	83 (119/144)	<0.001

Note: Data in parentheses are numbers from which the percentages were derived. T2WI, T2-weighted imaging; DCEI, dynamic contrast-enhanced imaging; DWI, diffusion-weighted imaging; PPV, positive predictive value; NPV, negative predictive value

* P values were calculated by comparing T2WI and DCEI

† P values were calculated by comparing T2WI and DWI

¶ P values were calculated by comparing T2WI and combined DCEI and DWI

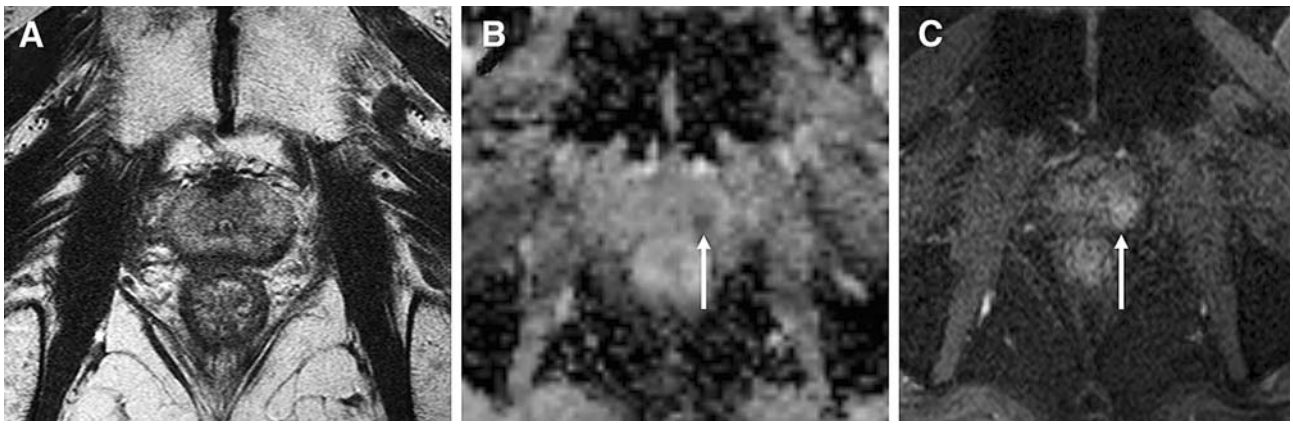

Fig. 1. A 73-year-old patient had increasing PSA levels 16 months after completion of radiation therapy. **A** An axial T2-weighted (3364/80) turbo spin–echo image shows diffusely low-signal intensity, representing radiation-induced changes. **B** However, the axial apparent diffusion coefficient map image shows a focal low-signal lesion (arrow) in the left peripheral zone of the midgland, which may represent a recurred cancer. **C** An axial dynamic contrast-enhanced image using a 3D-fast field echo sequence (7.4/3.9) shows an early well-enhancing lesion (arrow) in the corresponding site with B. At the subsequent transrectal ultrasound-guided biopsy, a recurred cancer focus with a Gleason score of eight was found in the left peripheral zone of the midgland.

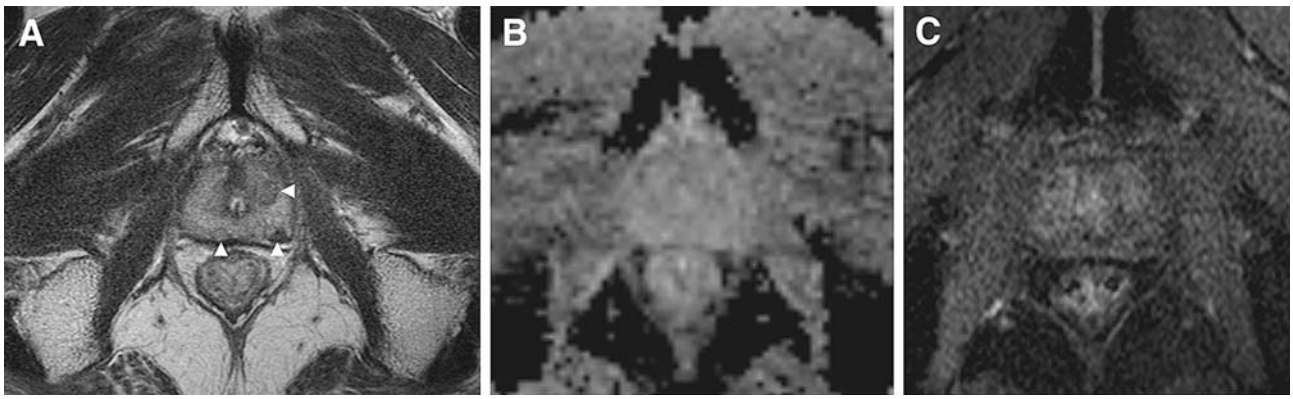

Fig. 2. A 67-year-old patient had increased PSA levels 24 months after completion of external beam radiation therapy. **A** An axial T2-weighted (3368/80) turbo spin–echo image shows three nodular lesions of low signal intensity in both peripheral zones of the midgland (arrowheads), suggesting the possibility of recurrent cancer. **B–C** However, the axial apparent diffusion coefficient map image (**B**) and axial dynamic contrast-enhanced image (**C**) using a 3D-fast field echo sequence (7.4/3.9) show no demonstrable mass. At a subsequent transrectal ultrasound-guided biopsy, no recurred cancer foci were found.

DWI is based on the diffusion motion of water protons in the tissues. When the measuring molecular motion with DWI, only the ADC can be calculated [22, 23]. ADC values of biological tissue are determined by many factors [24]. The motion of the protons is restricted by such barriers as membranes, organelles, the cytoskeleton, and macromolecules inside different tissue compartments. In addition, the size and number of mobile protons in these compartments can vary. After radiation therapy, malignant tumors of the brain, head and neck, and musculoskeletal system have enlarged nuclei and show hypercellularity compared with post-treatment changes [25–27]. These histological characteristics reduce the diffusion space of water protons in both the extracellular and intracellular environment with a resultant decrease in the ADC values. In this study, the diagnostic criteria of recurrent prostate cancer for DWI after radiation therapy were defined when focal low-signal intensity relative to the surrounding prostate tissue on ADC maps (i.e., low ADC values compared to surrounding prostate tissue) was identified. Our study results demonstrated better accuracy for DWI than T2WI in predicting locally recurrent prostate cancer after radiation therapy. With respect to recurrent prostate cancer after radiation therapy, the cause of the decreased ADC values relative to the surrounding irradiated benign

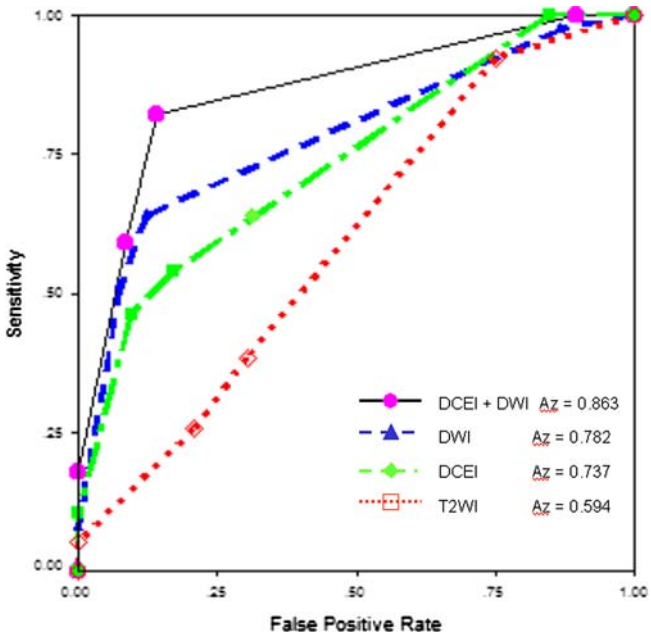

Fig. 3. Receiver operating characteristic curves show the results of the interpretation of T2-weighted (T2WI), dynamic contrast-enhanced (DCEI), diffusion-weighted (DWI), and combined DCEI and DWI. A significantly greater Az was determined for combined DCEI and DWI (Az = 0.863, $P < 0.05$), as compared with T2WI, DCEI, and DWI.

tissue is still unknown, but a possible cause might be the same mechanism as that responsible for the decreased ADC values of malignant tumors of the brain and head and neck. A further histological investigation is necessary to determine the cause conclusively. A recent study reported that after radiation therapy, ADC values of prostate cancer increased significantly compared with noncancerous tissue and thus, a significant difference between prostate cancer and noncancerous tissue had disappeared [28].

In this study, for predicting locally recurrent cancer after radiation therapy, the sensitivity of combined DCEI and DWI was observed to be slightly greater than that of either DWI or DCEI alone, but there was not any statistical significant difference. For predicting locally recurrent cancer after radiation therapy, a significantly greater Az was determined for combined DCEI and DWI (Az = 0.863), as compared with T2WI, DCEI, and DWI. Therefore, our results suggest that the use of combined DCEI and DWI may be more useful than the use of either DCEI or DWI alone for the prediction of locally recurrent cancer after radiation therapy.

There are several limitations to this study. The main limitation was that the transrectal biopsy results were used as the standard of reference. In this study, although the extended method (more than ten biopsy sites) of TRUS-guided biopsy was used, it is subject to sampling error and the histopathological interpretation of tissue from the irradiated prostate is difficult [29]. Postradiation therapy biopsy results may be false-negative due to sampling error or false-positive due to delayed tumor progression, but positive results of postradiation therapy biopsies are independent predictors of treatment outcome [29]. Owing to the high morbidity associated with surgery, our institution does not perform salvage prostatectomy but rather performs adjuvant hormonal manipulation or transrectal high-intensity-focused ultrasound for locally recurred prostate cancer after radiation therapy. Therefore, first, we have used the extended sextant biopsy results as the standard of reference. Second, this study had a small inhomogeneous population; five of 24 patients underwent adjuvant hormonal therapy after radiation therapy. Third, the study was a retrospective analysis. And finally, no endorectal coil was used in this study.

In conclusion, for the prediction of locally recurrent prostate cancer in patients with biochemical failure after external beam radiation therapy, our preliminary results suggest that 3T prostate MR imaging using a phased-array coil may be a feasible technique and that the use of either DWI or DCEI are superior to the use of T2WI.

References

1. Shipley WU, Thames HD, Sandler HM, et al. (1999) Radiation therapy for clinically localized prostate cancer: a multi-institutional pooled analysis. Jama 281:1598–1604
2. Lee WR, Moughan J, Owen JB, Zelefsky MJ (2003) The 1999 patterns of care study of radiotherapy in localized prostate carcinoma: a comprehensive survey of prostate brachytherapy in the United States. Cancer 98:1987–1994
3. Grado GL, Collins JM, Kriegshauser JS, et al. (1999) Salvage brachytherapy for localized prostate cancer after radiotherapy failure. Urology 53:2–10
4. Stephenson AJ, Scardino PT, Bianco FJ Jr, Eastham JA (2004) Salvage therapy for locally recurrent prostate cancer after external beam radiotherapy. Curr Treat Options Oncol 5:357–365
5. Shekarriz B, Upadhyay J, Pontes JE (2001) Salvage radical prostatectomy. Urol Clin North Am 28:545–553
6. Boccon-Gibod L, Djavan WB, Hammerer P, et al. (2004) Management of prostate-specific antigen relapse in prostate cancer: a European Consensus. Int J Clin Pract 58:382–390
7. Coakley FV, Hricak H, Wefer AE, et al. (2001) Brachytherapy for prostate cancer: endorectal MR imaging of local treatment-related changes. Radiology 219:817–821
8. Rouviere O, Valette O, Grivolat S, et al. (2004) Recurrent prostate cancer after external beam radiotherapy: value of contrast-enhanced dynamic MRI in localizing intraprostatic tumor—correlation with biopsy findings. Urology 63:922–927
9. Pucar D, Shukla-Dave A, Hricak H, et al. (2005) Prostate cancer: correlation of MR imaging and MR spectroscopy with pathologic findings after radiation therapy-initial experience. Radiology 236:545–553
10. Heijmink SW, Scheenen TW, Futterer JJ, et al. (2007) Prostate and lymph node proton magnetic resonance (MR) spectroscopic imaging with external array coils at 3 T to detect recurrent prostate cancer after radiation therapy. Invest Radiol 42:420–427
11. Sala E, Akin O, Moskowitz CS, et al. (2006) Endorectal MR imaging in the evaluation of seminal vesicle invasion: diagnostic accuracy and multivariate feature analysis. Radiology 238:929–937
12. Pickett B, Kurhanewicz J, Coakley F, et al. (2004) Use of MRI and spectroscopy in evaluation of external beam radiotherapy for prostate cancer. Int J Radiat Oncol Biol Phys 60:1047–1055
13. Futterer JJ, Scheenen TW, Heijmink SW, et al. (2007) Standardized threshold approach using three-dimensional proton magnetic

resonance spectroscopic imaging in prostate cancer localization of the entire prostate. Invest Radiol 42:116–122
14. Kim CK, Park BK (2008) Update of prostate magnetic resonance imaging at 3 T. J Comput Assist Tomogr 32:163–172
15. Tanenbaum LN (2006) Clinical 3T MR imaging: mastering the challenges. Magn Reson Imaging Clin N Am 14:1–15
16. Manenti G, Carlani M, Mancino S, et al. (2007) Diffusion tensor magnetic resonance imaging of prostate cancer. Invest Radiol 42:412–419
17. Kim CK, Park BK, Lee HM, Kwon GY (2007) Value of diffusion-weighted imaging for the prediction of prostate cancer location at 3T using a phased-array coil: preliminary results. Invest Radiol 42:842–847
18. American Society for Therapeutic Radiology, Oncology Consensus Panel (1997) Consensus statement: guidelines for PSA following radiation therapy. Int J Radiat Oncol Biol Phys 37:1035–1041
19. Huisman HJ, Engelbrecht MR, Barentsz JO (2001) Accurate estimation of pharmacokinetic contrast-enhanced dynamic MRI parameters of the prostate. J Magn Reson Imaging 13:607–614
20. Kim CK, Park BK, Kim B (2006) Localization of prostate cancer using 3T MRI: comparison of T2-weighted and dynamic contrast-enhanced imaging. J Comput Assist Tomogr 30:7–11
21. Futterer JJ, Heijmink SW, Scheenen TW, et al. (2006) Prostate cancer localization with dynamic contrast-enhanced MR imaging and proton MR spectroscopic imaging. Radiology 241:449–458
22. Schaefer PW, Grant PE, Gonzalez RG (2000) Diffusion-weighted MR imaging of the brain. Radiology 217:331–345
23. Lichy MP, Aschoff P, Plathow C, et al. (2007) Tumor Detection by Diffusion-Weighted MRI and ADC-Mapping-Initial Clinical Experiences in Comparison to PET-CT. Invest Radiol 42:605–613
24. Schaefer PW, Ozsunar Y, He J, et al. (2003) Assessing tissue viability with MR diffusion and perfusion imaging. AJNR Am J Neuroradiol 24:436–443
25. Abdel Razek AA, Kandeel AY, Soliman N, et al. (2007) Role of diffusion-weighted echo-planar MR imaging in differentiation of residual or recurrent head and neck tumors and posttreatment changes. AJNR Am J Neuroradiol 28:1146–1152
26. Hein PA, Eskey CJ, Dunn JF, Hug EB (2004) Diffusion-weighted imaging in the follow-up of treated high-grade gliomas: tumor recurrence versus radiation injury. AJNR Am J Neuroradiol 25:201–209
27. Baur A, Huber A, Arbogast S, et al. (2001) Diffusion-weighted imaging of tumor recurrences and posttherapeutical soft-tissue changes in humans. Eur Radiol 11:828–833
28. Takayama Y, Kishimoto R, Hanaoka S, et al. (2008) ADC value and diffusion tensor imaging of prostate cancer: changes in carbon-ion radiotherapy. J Magn Reson Imaging 27:1331–1335
29. Crook J, Malone S, Perry G, et al. (2000) Postradiotherapy prostate biopsies: what do they really mean? Results for 498 patients. Int J Radiat Oncol Biol Phys 48:355–367